Identification of a New Class of Inhibitors of the Voltage-Gated Potassium Channel, $K_v1.3$, with Immunosuppressant Properties†

William A. Schmalhofer,‡,§ Jianming Bao,‡,‖ Owen B. McManus,‡,§ Brian Green,§ Mary Matyskiela,§ Denise Wunderler,§ Randal M. Bugianesi,§ John P. Felix,§ Markus Hanner,§,# Ana-Rosa Linde-Arias,§ Cristiano G. Ponte,§ Lucia Velasco,§ Gloria Koo,⊥ Mary Jo Staruch,⊥ Shouwu Miao,‖ William H. Parsons,‖ Kathleen Rupprecht,‖ Robert S. Slaughter,§ Gregory J. Kaczorowski,§ and Maria L. Garcia*,§

Departments of Ion Channels, Medicinal Chemistry, and Immunology Research, Merck Research Laboratories, P.O. Box 2000, Rahway, New Jersey 07065

Received February 22, 2002; Revised Manuscript Received April 26, 2002

ABSTRACT: The voltage-gated potassium channel, $K_v1.3$, is a novel target for development of immunosuppressants. Using a functional $^{86}Rb^+$ efflux assay, a new class of high-affinity $K_v1.3$ inhibitors has been identified. The initial active in this series, 4-phenyl-4-[3-(2-methoxyphenyl)-3-oxo-2-azaprop-1-yl]cyclohexanone (PAC), which is representative of a disubstituted cyclohexyl (DSC) template, displays a K_i of ca. 300 nM and a Hill coefficient near 2 in the flux assay and in voltage clamp recordings of $K_v1.3$ channels in human T-lymphocytes. PAC displays excellent specificity as it only blocks members of the K_v1 family of potassium channels but does not affect many other types of ion channels, receptors, or enzyme systems. Block of $K_v1.3$ by DSC analogues occurs with a well-defined structure−activity relationship. Substitution at the C-1 ketone of PAC generates trans (down) and cis (up) isomer pairs. Whereas many DSC derivatives do not display selectivity in their interaction with different $K_v1.x$ channels, trans DSC derivatives distinguish between $K_v1.x$ channels based on their rates of C-type inactivation. DSC analogues reversibly inhibit the Ca^{2+}-dependent pathway of T cell activation in in vitro assays. Together, these data suggest that DSC derivatives represent a new class of immunosuppressant agents and that specific interactions of trans DSC analogues with channel conformations related to C-type inactivation may permit development of selective $K_v1.3$ channel inhibitors useful for the safe treatment of autoimmune diseases.

The voltage-gated potassium channel, $K_v1.3$,[1] plays a crucial role in human T-lymphocyte activation (*1*, *2*). In human T cells, $K_v1.3$ channels exist as tetramers of four identical subunits (*3*) and control the resting membrane potential of the cell (*4*). Inhibition of $K_v1.3$ channels causes T cell depolarization. This leads to an attenuation of the rise in intracellular Ca^{2+} concentration that occurs upon cell stimulation, which is required to drive T cell activation (*5*). Peptidyl blockers of $K_v1.3$ channels, such as margatoxin (MgTX) (*6*) and kaliotoxin (*7*), have immunosuppressant activity in vivo. These animal data suggest that $K_v1.3$ represents a therapeutic target for treating autoimmune diseases.

Efforts have been directed toward the identification of small molecules that selectively block $K_v1.3$ channels. A novel nortriterpene, correolide, was isolated from the plant *Spachea correa* and shown to be a potent $K_v1.3$ channel blocker (*8*, *9*). Correolide binds with a 1:1 stoichiometry to $K_v1.3$ channels and is a selective inhibitor of the K_v1 family of potassium channels (*9*). Members of the correolide family of $K_v1.3$ channel inhibitors mimic MgTX in in vitro immunological assays using human T cells, and two analogues of correolide, with appropriate pharmacokinetic properties, suppress a delayed-type hypersensitivity response to tuberculin in vivo in mini-swine (*10*). However, correolide and its analogues also appear to inhibit $K_v1.1$ channels present in some peripheral nerve terminals (*11*), thereby causing acetylcholine release, which explains some of the limited toxicity observed in vivo with this structural series. The molecular complexity of correolide has hindered me-

† M.H. was a recipient of Erwin Schroedinger Fellowships J-01108-MED and J-01460-MED of the Austrian Research Foundation.

* To whom correspondence should be addressed. Phone: (732) 594-7564. Fax: (732) 594-3925. E-mail: maria_garcia@merck.com.

‡ Contributed equally to this work.

§ Department of Ion Channels, Merck Research Laboratories.

Present address: INTERCELL, Rennweg 95B, A-1030 Wien, Austria.

‖ Department of Medicinal Chemistry, Merck Research Laboratories.

⊥ Department of Immunology Research, Merck Research Laboratories.

[1] Abbreviations: K_v, voltage-gated potassium channel; PAC, 4-phenyl-4-[3-(2-methoxyphenyl)-3-oxo-2-azaprop-1-yl]cyclohexanone; DSC, disubstituted cyclohexyl; diTC, ditritiocorreolide; diHC, dihydrocorreolide; ^{125}I-HgTX$_1$A19Y/Y37F, monoiodotyrosine−hongotoxin$_1$−A19Y/Y37F; MgTX, margatoxin; K_d, equilibrium dissociation constant; K_i, equilibrium inhibition constant; PBMC, peripheral blood mononuclear cells; IL-2, interleukin 2.

10.1021/bi025722c CCC: $22.00
Published on Web 05/24/2002

dicinal chemistry efforts to identify an analogue with appropriate characteristics for clinical development. Other small molecule inhibitors of $K_v1.3$, such as UK-78282 (*12*), WIN 17317-3 (*13*, *14*), and verapamil (*15*, *16*), have been described. However, neither WIN 17317-3 nor verapamil appear to be viable drug development candidates since they block, with high affinity, voltage-gated sodium or calcium channels, respectively (*17*).

The search for novel $K_v1.3$ channel inhibitors has led to the identification of a new class of channel blockers. The parent compound, 4-phenyl-4-[3-(2-methoxyphenyl)-3-oxo-2-azaprop-1-yl]cyclohexanone (PAC), a disubstituted cyclohexyl (DSC) analogue, blocks $K_v1.3$ channels in functional assays, inhibits diTC binding to $K_v1.x$ channels, and suppresses the Ca^{2+}-dependent pathway of T cell activation in in vitro assays. The structure−activity relationship for inhibition of $K_v1.3$ channels by DSC analogues is well-defined. Synthesis of trans (down) and cis (up) isomers at the C-1 cyclohexyl position yields DSC derivatives that display a differential interaction with $K_v1.x$ channels, and the trans DSC isomers are more selective inhibitors of ditritiocorreolide (diTC) binding to $K_v1.3$ than to native brain $K_v1.x$ channels. These data identify a new class of immunosuppressant agents and suggest that high-affinity interaction of trans DSC derivatives preferentially occurs to channel conformations specific for $K_v1.3$ channels and which may be coupled to C-type inactivation. The specificity of this interaction and the simplicity of the DSC template create possibilities for developing selective $K_v1.3$ channel inhibitors useful as immunosuppressants.

EXPERIMENTAL PROCEDURES

Materials. Restriction enzymes and the pCI-neo vector were bought from Promega. The pEGFP-N1 vector was from Clontech and *Pfu* DNA polymerase from Stratagene. The TsA-201 cell line, a subclone of the human embryonic kidney cell line HEK293 that expresses the SV40 T antigen, was a gift of Dr. Robert DuBridge. All tissue culture media were from Gibco, serum was from Hyclone, and the FuGENE6 transfection reagent was from Roche. ^{86}RbCl and [^{3}H]thymidine (6.7 Ci/mmol) were purchased from NEN Life Science Products. CHO cells stably transfected with $K_v1.3$ were prepared as previously described (*3*). HEK293 cells stably transfected with either homotetrameric $K_v1.1$, $K_v1.3$, $K_v1.4$, $K_v1.5$, or $K_v1.6$ channels were obtained from Professor Olaf Pongs (Zentrum für Molekulare Neurobiologie, Hamburg, Germany), while HEK293 cells stably transfected with $K_v1.2$ were prepared as described (*18*). Human brain tissue was provided by Drs. H.-G. Knaus and H. Glossmann, University of Innsbruck, Austria. Correolide, diTC (29 Ci/mmol), and dihydrocorreolide (diHC) were prepared as previously described (*9*). Hongotoxin$_1$-A19Y/Y37F (HgTX$_1$A19Y/Y37F) was prepared and radioiodinated using literature procedures (*19*). Human T cell conditioned medium was from Collaborative Research, Cambridge, MA. OKT3 (anti-CD3) mAb was obtained from Ortho Diagnostic Systems (Raritan, NJ). GF/C glass fiber filters were obtained from Whatman, and poly(ethylenimine) was from Sigma. All other reagents were obtained from commercial sources and were of the highest purity commercially available.

*Synthesis of 4-Phenyl-4-[3-(2-methoxyphenyl)-3-oxo-2-azaprop-1-yl]cyclohexanone (PAC) and Derivatives. (A) Preparation of Amide **4**:*

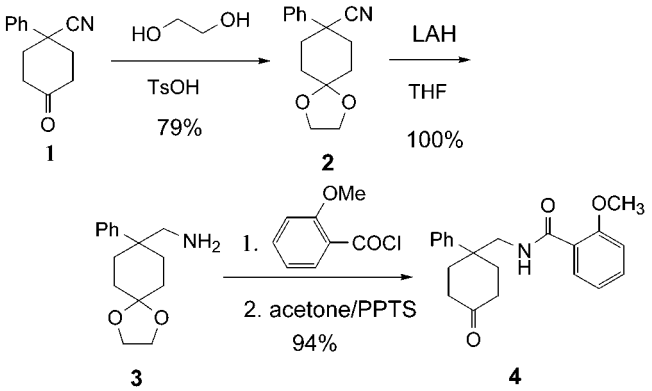

*Step 1 (Compound **2**).* A solution of 4.01 g (20.1 mmol) of 4-cyano-4-phenylcyclohexanone, 10 mL of ethylene glycol, and 0.072 g of *p*-toluenesulfonic acid monohydrate in 40 mL of benzene was heated at reflux for 18 h, and the water formed during the reaction was removed via a Dean−Stark distillation receiver. The reaction mixture was placed under reduced pressure to remove the solvent, and the residue was poured into 200 mL of ether. It was washed with water (20 mL × 3), dried over $MgSO_4$, and concentrated. The residue was purified by flash chromatography using EtOAc/hexane (1:6) to afford 3.88 g of compound **2** as a white solid (79%).

*Step 2 (Compound **3**).* To a suspension of 3.88 g (16.0 mmol) of compound **2** in 40 mL of dry THF was added slowly 32 mL of lithium aluminum hydride (1.0 M in THF, 32 mmol), and the reaction was treated at reflux for 3.4 h. TLC analysis showed no starting material, and the reaction mixture was cooled to 0 °C. Then it was quenched with 4 mL of 4 N NaOH at 0 °C, filtered through a plug of Na_2SO_4, and concentrated to give 4.00 g of compound **3** as a colorless oil (100%).

*Step 3 (Compound **4**).* To a solution of 1.14 g (4.62 mmol) of compound **3** and 1.3 mL of triethylamine (9.33 mmol) in 20 mL of methylene chloride was added 1.4 mL (9.33 mmol) of *o*-anisoyl chloride at room temperature. The reaction mixture was stirred for 15 h and was poured into 200 mL of ether. It was washed with aqueous $NaHCO_3$, dried over $MgSO_4$, and concentrated. The residue was dissolved in 15 mL of acetone and pyridinium *p*-toluenesulfonate (114 mg), and 1.5 mL of water was added. The solution was heated at reflux for 4 h and was then removed of volatiles. The residue was purified by flash chromatography to afford 1.65 g of compound **4** (PAC) as a white solid (94%): ^{1}H NMR (500 MHz, $CDCl_3$) δ 2.13 (m, 1H), 2.32 (m, 1H), 2.46−2.54 (m, 2H), 3.64 (m, 3H), 3.78 (d, 2H, J = 5.9 Hz), 6.89 (d, 1H, J = 8.2 Hz), 7.06 (t, 1H, J = 7.1 Hz), 7.36 (t, 1H, J = 6.8 Hz), 7.41 (t, 1H, J = 7.5 Hz), 7.46−7.51 (m, 4H), 7.68 (br s, 1H), 8.19 (d, 1H, J = 7.8 Hz); mass spectrum (PB-NH_3/CI) *m*/*e* 338 (M + 1). Other compounds in Table 1 were prepared similarly.

*(B) Preparation of Alcohols **5** and **6**:*

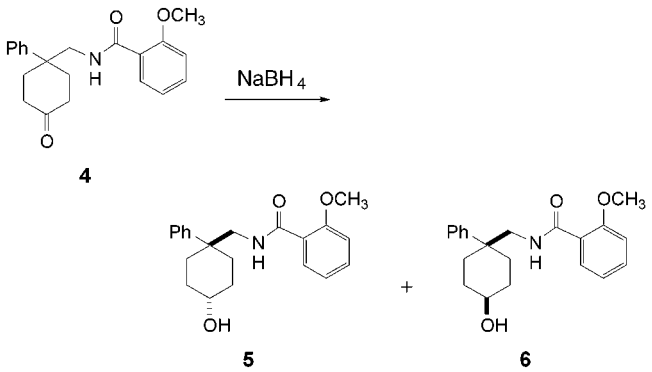

To a solution of 1 g (2.97 mmol) of compound **4** in 30 mL of THF was added slowly 224 mg (5.93 mmol) of $NaBH_4$ at room temperature. The reaction mixture was stirred at room temperature for 5 h and was poured into 30 mL of methylene chloride. It was washed with 10 mL of 1 N HCl, dried over $MgSO_4$, and concentrated. The residue was purified by silica gel chromatography with methylene chloride/*tert*-butyl methyl ether to afford 340 mg of compound **5** as a white solid and 540 mg of compound **6** as a white solid (trans:cis = 1:1.6).

Compound **5**: ^{1}H NMR (500 MHz, $CDCl_3$) δ 1.37 (m, 2H), 1.63 (m, 2H), 1.89 (m, 2H), 2.39 (m, 2H), 3.62 (d, 2H, J = 6 Hz), 3.64 (s, 3H), 3.77 (m, 1H), 6.88 (d, 1H, J = 8 Hz), 7.05 (t, 1H, J = 7.5 Hz), 7.29 (t, 1H, J = 5.8 Hz), 7.38−7.45 (m, 5H), 7.57 (br s, 1H), 8.20 (d, 1H, J = 7.7 Hz); mass spectrum (PB-NH_3/CI) *m/e* 340 (M + 1). Compound **6**: ^{1}H NMR (500 MHz, $CDCl_3$) δ 1.75−2.16 (m, 8H), 3.58 (s, 3H), 3.76 (m, 1H), 3.80 (d, 2H, J = 6 Hz), 6.85 (d, 1H, J = 8 Hz), 7.05 (t, 1H, J = 8 Hz), 7.29 (t, 1H, J = 6.9 Hz), 7.39−7.46 (m, 5H), 7.56 (s, 1H), 8.21 (d, 1H, J = 7.8 Hz); mass spectrum (PB-NH_3/CI) *m/e* 340 (M + 1).

*(C) Preparation of Compound **8**:*

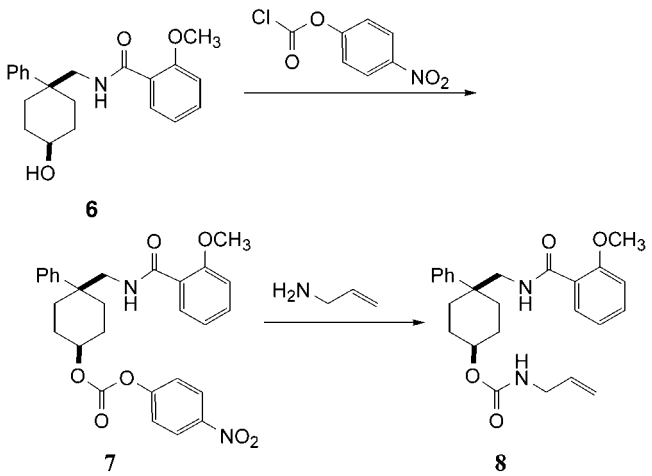

*Step 1 (Compound **7**).* A solution of 105 mg (0.31 mmol) of compound **6**, 112 mg (0.56 mmol) of 4-nitrophenyl chloroformate, and 94 mg (0.93 mmol) of triethylamine in 10 mL of dichloromethane was stirred at room temperature for 3 h. Then the reaction mixture was concentrated, and the residue was purified by silica gel chromatography with hexane/ethyl acetate to afford 124 mg of compound **7** as a white solid (80%): ^{1}H NMR (500 MHz, $CDCl_3$) δ 1.84 (m, 1H), 2.02−2.16 (m, 6H), 3.61 (s, 3H), 3.77 (d, 2H, J = 6.0 Hz), 4.85 (m, 1H), 6.88 (d, 1H, J = 8.3 Hz), 7.07 (t, 1H, J = 7.5 Hz), 7.33 (m, 1H), 7.40−7.46 (m, 7H), 8.23 (d, 1H, J = 8.0 Hz), 8.31 (d, 2H, J = 8 Hz); mass spectrum (PB-NH_3/CI) *m/e* 505.2 (M + 1).

*Step 2 (Compound **8**).* To a solution of 30 mg (0.061 mmol) of compound **7** in 5 mL of dichloromethane was added 100 mg (1.75 mmol) of allylamine at room temperature. The reaction mixture was stirred for 2 h. Then it was concentrated and purified by silica gel chromatography with hexane/ethyl acetate (2:1) to afford 36 mg of compound **8** as a white solid (100%): ^{1}H NMR (500 MHz, $CDCl_3$) δ 1.25−2.03 (m, 8H), 3.58 (s, 3H), 3.74 (d, 2H, J = 6 Hz), 3.82 (t, 2H, J = 6 Hz), 4.75 (br s, 1H), 4.82 (br s, 1H), 5.16 (d, 1H, J = 11 Hz), 5.24 (d, 1H, J = 19 Hz), 5.89 (m, 1H), 6.86 (d, 1H, J = 8.2 Hz), 7.05 (t, 1H, J = 7.1 Hz), 7.30 (m, 1H), 7.38−7.45 (m, 5H), 7.56 (br s, 1H), 8.21 (d, 1H, J = 7.8 Hz); mass spectrum (PB-NH_3/CI) *m/e* 423 (M + 1). Other compounds in Table 2 were prepared using the same method from either **5** or **6**.

Human T Cell Preparation. Human peripheral blood mononuclear cells (PBMC) were isolated as previously indicated (*10*). Purified T cells were prepared by rosetting as described (*10*). Purity of human T cells was 95−97%, as determined by anti-CD3 staining in FACS analyses.

$^{86}Rb^+$ Efflux Assay. $^{86}Rb^+$ efflux from CHO cells stably expressing $K_v1.3$ was performed as previously described (*9*). Test compounds were preincubated with cells for 10 min in low potassium buffer (in mM: 4.6 KCl, 126.9 NaCl, 1 $CaCl_2$, 2 $MgCl_2$, and 10 Hepes, pH 7.2, adjusted with NaOH). $^{86}Rb^+$ efflux was initiated by depolarization of the cells with high potassium buffer (final concentration, in mM: 63.25 KCl, 69.2 NaCl, 1 $CaCl_2$, 2 $MgCl_2$, and 10 Hepes, pH 7.2, adjusted with NaOH) in the presence of compound. Activity was determined as percent inhibition of $^{86}Rb^+$ efflux that is sensitive to 50 nM MgTX.

Electrophysiology. Whole cell recordings were made from purified human T-lymphocytes as previously described (*10*) using standard methods (*20*). Electrodes were pulled from Garner 7052 glass and their resistances were 1−4 mΩ. For whole cell experiments, the pipet contained (mM) 140 KCl, 10 Hepes, and 10 K_2EGTA, pH 7.2, with KOH, and the bath solution contained (mM) 160 NaCl, 10 Hepes, 4.5 KCl, 2 $CaCl_2$, and 1 $MgCl_2$, pH 7.2, with NaOH. On-cell and excised inside-out patch recordings were made from CHO cells stably expressing $K_v1.3$ channels or from CHO cells transiently transfected with different $K_v1.x$ DNAs. In the patch experiments, the pipet contained the 160 mM NaCl bath solution described above. The electrode was zeroed in this bath solution, and after seal formation, the bath was switched to the 140 mM KCl solution described above to clamp the cell membrane potential near 0 mV. In some cases, chloride was replaced with fluoride to increase stability of excised patches. The amplifier inputs were connected to the experimental solutions via $Ag/AgCl_2$ electrodes, and the bath electrode used an agar bridge containing 200 mM KCl. No corrections for junction potentials or series resistance were applied. Experiments were done under constant flow (1−2 mL/min) with a chamber volume of 0.2−0.4 mL at room temperature (22−24 °C).

Membrane currents were measured with Axopatch 1D (Axon Instruments) or EPC9 (HEKA Electronik) amplifiers. Voltage control and data acquisition were done using ITC-16 interfaces (Instrutech Corp.) connected to MacIntosh

computers (Apple Computers) running Pulse software (HEKA Electronik). Currents were filtered at 2−5 kHz and digitized at 5−10 kHz. Analogue capacity compensation was applied, and digital compensation of the leak and residual capacity currents was done using a P/−4 protocol from the standard holding potential (−80 mV), with subtraction pulses applied 4−10 s after the test pulses.

Mutant Channel Constructs. A 9E10 c-myc tag was introduced at the C-terminus of $K_v1.3$ using an oligonucleotide cassette containing *Hin*dIII and *Not*I restriction sites. Chimeric cDNAs were generated using the gene splicing with overlap extension technique (*21*). Chimeras were constructed as follows: in $K_v1.1-pK_v1.3$, the linker between transmembrane domains S_5 and S_6 of $K_v1.1$ was replaced with the corresponding region of $K_v1.3$, whereas in $K_v1.3-pK_v1.2$, the linker of $K_v1.3$ was replaced with the corresponding one of $K_v1.2$ (*18*). Site-directed mutagenesis was performed using the overlap extension technique (*21*). Polymerase chain reaction was carried out using proof reading *Pfu* DNA polymerase, and the integrity of all constructs was verified by nucleotide sequencing (automated sequencer, ABI 377).

Transfection of CHO and TsA-201 Cells and Membrane Preparation. CHO cells were grown in MEM supplemented with defined fetal bovine serum, penicillin/streptomycin, and L-glutamine in 5% CO_2 at 37 °C. For transfection, cells were seeded into T-225 cm^2 flasks at a density of 5×10^6 cells per flask and let to acclimate overnight. Cells were transfected using FuGENE6 transfection reagent, following the manufacturer's instructions, at a FuGENE6:DNA ratio of 3:1. For each T-225 cm^2 flask, 10 μg of the corresponding cDNA and 4 μg of green fluorescence cDNA were used. Transfected cells were identified under a fluorescence microscope 48 h after transfection. The procedures for handling TsA-201 cells, their transfection with FuGENE6 transfection reagent, and preparation of membranes have been previously described (*22*). Membrane vesicles derived from either HEK cells stably transfected with homomultimeric $K_v1.x$ channels or human brain tissue were prepared as previously indicated (*18*). The final membrane pellet was resuspended in 100 mM NaCl and 20 mM Hepes−NaOH, pH 7.4. Aliquots were frozen in liquid N_2 and stored at −70 °C.

^{125}I-HgTX$_1$A19Y/Y37F Binding. The interaction of ^{125}I-HgTX$_1$A19Y/Y37F with either $K_v1.x$ or brain membranes was measured in a medium consisting of 100 mM NaCl, 5 mM KCl, 20 mM Tris-HCl, pH 7.4, and 0.1% bovine serum albumin, in the absence or presence of increasing concentration of the test compound. Incubations were carried out in a total volume of 6 mL for 20 h at room temperature. Separation of bound from free ligand was achieved using filtration protocols as described (*23*).

DiTC Binding. Binding of diTC to $K_v1.x$-containing membranes was carried out in a medium consisting of 135 mM NaCl, 4.6 mM KCl, 20 mM Tris-HCl, pH 7.4, and 0.02% bovine serum albumin. Experiments were carried out in a total volume of 0.2 mL with 5 nM diTC in the absence or presence of increasing concentrations of diHC. Separation of bound from free ligand was achieved using a filtration protocol as described (*18*). Triplicate samples were determined for each experimental point. Standard deviation of the mean was typically less than 5%.

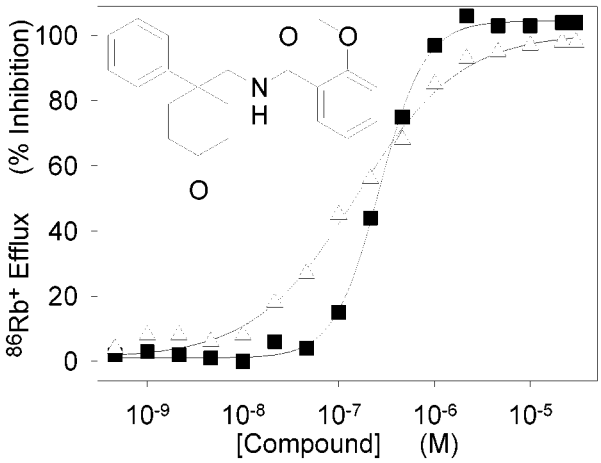

FIGURE 1: $^{86}Rb^+$ efflux from CHO/$K_v1.3$ cells. CHO cells stably transfected with $K_v1.3$ were loaded with $^{86}Rb^+$ and incubated in the absence or presence of increasing concentrations of either 4-phenyl-4-[3-(2-methoxyphenyl)-3-oxo-2-azaprop-1-yl]cyclohexanone (PAC) (■) or correolide (△). Efflux was initiated by addition of high potassium buffer in the presence of test compounds, and cells were incubated at room temperature for 15 min. Inhibition of $^{86}Rb^+$ efflux was assessed relative to the MgTX-sensitive component of an untreated control. The structure of PAC is illustrated.

Data Analysis. IC_{50} values for inhibition of diTC and ^{125}I-HgTX$_1$A19Y/Y37F binding were determined using the equation:

$$B_{eq} = (B_{max} - B_{min})/[1 + (I/IC_{50})^{n_H}] + B_{min}$$

where B_{eq} is the degree of binding at the ligand concentration tested with no inhibitors present, B_{min} is the minimum amount of ligand bound at higher concentrations of inhibitor where the binding curve has leveled off, I is the inhibitor concentration, n_H is the Hill coefficient, and IC_{50} is the inhibition constant. For the diTC data, B_{max} was usually around 100% and B_{min} was 0%.

Proliferation Assays. Purified T-lymphocytes were cultured in 96-well microtiter plates (Costar, Cambridge, MA) as described (*10*). Compounds were added and incubated for 15−30 min at 37 °C. The cultures were stimulated with 0.3 ng/mL OKT3. Irradiated (1500 R) autologous PBMC cells were then added, and cultures were incubated for 3 days at 37 °C, as described (*10*). T cell proliferation was measured by addition of 2 μCi/well [^{3}H]thymidine about 18 h before harvesting. Cultures were harvested, and radioactivity associated with filters was determined by liquid scintillation techniques. Data represent the means of triplicate wells.

RESULTS

Identification of a New Class of $K_v1.3$ Inhibitors. In the search for novel inhibitors of the $K_v1.3$ channel, 4-phenyl-4-[3-(2-methoxyphenyl)-3-oxo-2-azaprop-1-yl]cyclohexanone (PAC) was identified in a functional assay that monitors $^{86}Rb^+$ efflux from CHO cells stably transfected with $K_v1.3$ (Figure 1). PAC blocks the MgTX-sensitive component of the efflux reaction with an IC_{50} value of 273 ± 30 nM ($n = 12$). By comparison, correolide, a natural product $K_v1.3$ channel inhibitor (*9*, *10*), displays an IC_{50} of 149 ± 38 nM ($n = 13$) in this functional assay. The Hill coefficient for inhibition of $^{86}Rb^+$ flux by PAC is >1 and close to 2.

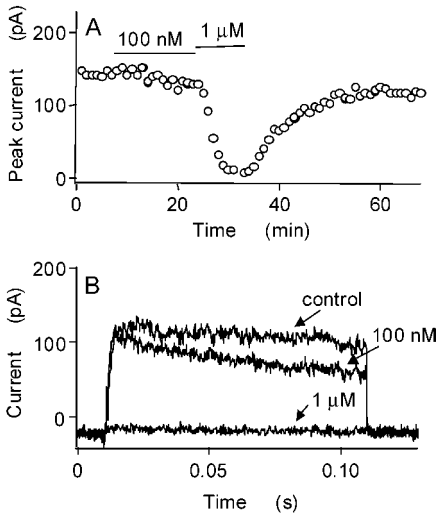

FIGURE 2: PAC reversibly blocks $K_v1.3$ channels in human T-lymphocytes. Whole cell currents were recorded from a human T-lymphocyte held at −80 mV and pulsed to +20 mV for 100 ms once per minute. Peak current amplitudes are plotted against time in (A), and individual traces are shown in (B) for control, 100 nM, and 1 μM PAC.

This is in marked contrast to correolide and analogues of correolide that consistently display Hill coefficients of 1 in this assay.

Block of the Voltage-Gated Potassium Channel, $K_v1.3$, in Human T-Lymphocytes. Voltage-gated potassium currents in human T-lymphocytes were measured by whole cell recording (*20*). Bath application of PAC reversibly blocked potasium currents evoked by brief (100 ms) depolarizations (Figure 2). The peak current was slightly suppressed by 100 nM PAC and was completely blocked by 1 μM PAC. The time course of the current activated during a depolarizing pulse was modified in the presence of 100 nM PAC (Figure 2B), with more block occurring at the end of the depolarizing pulse than at the beginning. After washout of PAC, the amplitude of the peak currents recovered along an exponential time course with a time constant of 8.6 min, indicating a slow rate of dissociation under these experimental conditions.

The change in kinetics of potassium currents caused by PAC in Figure 2 suggests that PAC might preferentially bind to specific states or conformations of the potassium channel. A dual pulse protocol was used to test for state-dependent channel block by PAC. A 1 s depolarizing pulse to +20 mV, which opened and fully inactivated the channels, was followed by a 60 s rest period at −80 mV to allow full recovery from inactivation and then followed by another 1 s pulse to +20 mV. This dual pulse sequence was repeated every 10 min. If channel block by PAC is indifferent to channel state, then the currents elicited by the second pulse should be blocked to the same degree as the first. In control (Figure 3A), the currents measured during pulse 1 and pulse 2 were nearly identical. The cell was then exposed to 3 μM PAC for 9 min, while held at −80 mV, at which voltage all channels would remain closed, and the dual pulse sequence was repeated in the presence of PAC (Figure 3B). On the basis of the time course of channel block after exposure to 1 μM PAC in Figure 2, complete block of both pulses would be expected, unless channel block was state-dependent. However, the peak current during pulse 1 was only reduced 19%, while the current during pulse 2 was completely blocked, suggesting state-dependent channel block by PAC. Overlaying the currents recorded during pulse 1 in control and in 3 μM PAC (Figure 3F), shows that although 3 μM PAC caused only a small decrease in the peak current, it produced a pronounced change in the time course of current decay during the depolarizing pulse, shortening the exponential time constant of decay from 228 to 47 ms. Current decay in control reflects entry into inactivated channel states (*24*, *25*), while, in PAC, current decay presumably results from entry into both inactivated and drug-blocked states. The small pedestal of noninactivated current remaining at the end of a 1 s pulse is completely blocked by PAC (Figure 3F).

After washout of PAC, the peak currents during pulse 1 and pulse 2 returned, in parallel, to control values with a time course of recovery similar to that observed in Figure 2 with continuous pulsing. These data suggest that depolarizing pulses are not necessary to allow PAC dissociation from channels. Notice that at 9 min of washout (20 min total time) the time constants of current decay had returned to control values, while the peak currents were still reduced by about half (0.48 and 0.46 for pulses 1 and 2, respectively). This observation, along with the single exponential rate of channel closing in all concentrations of PAC, is consistent with a mechanism where PAC directly blocks open channels.

The dual pulse protocol shown in Figure 3 was repeated at various concentrations of PAC, and results are shown in Figure 4. A single set of measurements was obtained for each cell, in control, and after 9 min exposure to a single concentration of PAC, and currents from four cells are plotted in Figure 4A−D. Two effects on the currents are apparent as the concentration of PAC is raised. First, the peak value of currents during the second pulse is reduced at much lower concentrations than those needed to block the peak currents during the first pulse. Averaged values for block of pulse 1 and pulse 2 from a number of cells were fit with a Hill equation (Figure 4E), giving an estimated K_i of 310 nM and a slope of 1.9 for block of pulse 2. This K_i value likely substantially underestimates the actual binding affinity to the preferred channel conformation as the measurements were made following a single 1 s depolarizing pulse. The Hill slope of 1.9 suggests that more than one PAC molecule can contribute to blocking a single channel. Block of pulse 1 by PAC occurred at higher concentrations than block of pulse 2 (Figure 4E). A K_i for block of pulse 1 could not be accurately estimated as the maximal observed block was 30% at 10 μM. The line in Figure 4E plots a Hill equation fit to pulse 1 data with a K_i value of 17 μM, with the maximal value fixed to 1 and the slope fixed to 1. These data indicate that a single, 1 s, depolarizing pulse shifts the potency for channel block by PAC more than 50-fold.

The second prominent effect of PAC on potassium currents seen in Figure 4 is an increase in the rate of current decay during depolarizing pulses. In the presence of PAC, the currents decay during a maintained depolarization along single-exponential time courses that reflect channel entry into inactivated and drug-blocked states. The aggregate rate of closing was calculated from the inverse of the time constant of decay of pulse 1 and plotted as a function of PAC concentration in Figure 4F. The closing rate continues to increase as PAC concentration is raised, consistent with a simple model where binding of PAC to open channels causes

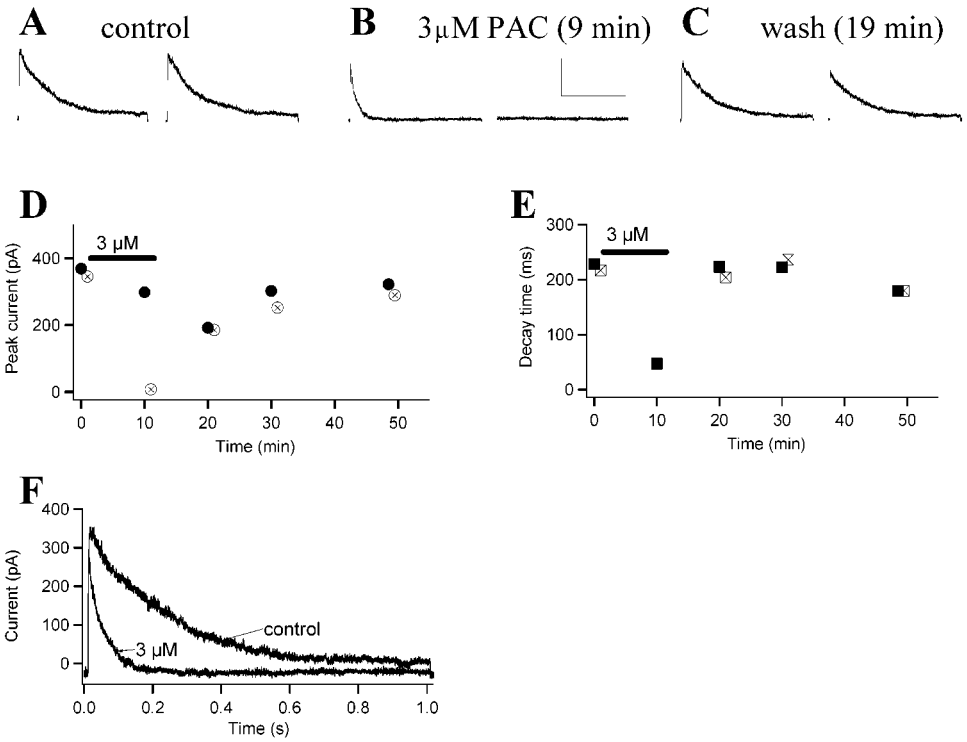

FIGURE 3: State-dependent block of $K_v1.3$ channels in human T-lymphocytes. A dual pulse protocol was used to test for state-dependent block of $K_v1.3$ channels by PAC. From a holding potential of −80 mV, a pair of 1 s pulses to +20 mV was separated by a 60 s recovery period at −80 mV. A pulse pair was delivered every 10 min. After two control pulses (A), the cell was exposed to 3 μM PAC for 10 min. The pulse pair recorded in the presence of PAC (9 min) is shown in (B) and after washout (19 min) in (C). The amplitudes of the peak currents from pulse 1 (●) and pulse 2 (○) are plotted in (D), and the time constants of decay for pulse 1 (■) and pulse 2 (□) are shown in (E). Pulse 1 in control and 3 μM PAC are overlaid in (F) to show the effects of PAC on the rate of current decay.

channel closure. The relationship between closing rate and PAC concentration was fit with a line (solid line). Assuming a simple model where channels can inactivate or be blocked in a bimolecular reaction by PAC from a single open state, the rate of PAC binding to open channels (1.1×10^7 M^{-1} s^{-1}) was estimated from the slope in Figure 4F. A power function of PAC concentration, with an exponent of 1.9 and a *y* intercept of 7.6 s^{-1}, gave an improved fit to the kinetic data shown in Figure 4F (not shown; log error ratio = −0.61), indicating that more than one PAC molecule can participate in channel block. The dashed line plots the closing rate as the square of PAC concentration with a *y* intercept of 7.8 s^{-1}, which also fit the kinetic data better than a line (log error ratio = −0.51). Analysis of both degree and kinetics of channel block by PAC suggests that two or more PAC molecules participate in channel block.

Access to the PAC Binding Site from the Intracellular Side. The location of the binding site on $K_v1.3$ channels for PAC will influence its ability to block channels. For instance, a membrane-impermeant compound that acts at the intracellular surface will not block in whole cell or on-cell experiments, where the compound is applied to the extracellular side of the membrane. As an initial approach toward localizing the binding site for PAC, different recording configurations were used to control access of PAC to either side of the membrane. For example, in whole cell recordings, bath-applied compounds have access to extracellular sites on the channels, and membrane-permeant compounds also have access to intracellular sites. In excised inside-out membrane patches, bath-applied compounds have direct access to intracellular sites. And, in on-cell patch recordings, bath-applied compounds do not have direct access to extracellular sites, but membrane-permeant compounds can access intracellular sites. Heterologous expression of $K_v1.3$ channels in CHO cells was used to generate high levels of expression, allowing recording of macroscopic currents from membrane patches.

Figure 5 shows recordings from on-cell and excised inside-out membrane patches from CHO cells expressing $K_v1.3$ channels. In all cases, the pipet contained high sodium, low potassium solution, and the bath contained a high potassium solution, so that the ionic gradients mimicked the conditions in the whole cell recordings shown in Figures 2−4. The patch-holding potential (−80 mV holding) is equal to the membrane potential in these conditions, and a series of pulses to +20 mV was applied to activate $K_v1.3$ channels. PAC reversibly blocked $K_v1.3$ channels in on-cell patches, suggesting that PAC is membrane permeant and acts at a site accessible from the cytoplasm side. PAC appears to be a more effective blocker when the pulse duration is increased from 100 ms to 1 s. When the on-cell patch shown in Figure 5C,D was excised into the inside-out configuration, PAC applied directly to the intracellular side also blocked $K_v1.3$ channels, confirming that the PAC site is accessible from the intracellular or membrane compartments.

The potency of PAC as a channel blocker in electrophysiological protocols is similar to that observed in the $^{86}Rb^+$ efflux assay and in ligand binding protocols (see below). Noteworthy is the fact that the Hill coefficient in both the flux and electrophysiology assays is close to 2. Such a profile suggests multiple inhibitor binding sites on each $K_v1.3$ channel.

Specificity Studies. The specificity of PAC against related ion channels, other superfamilies of ion channels, or unrelated

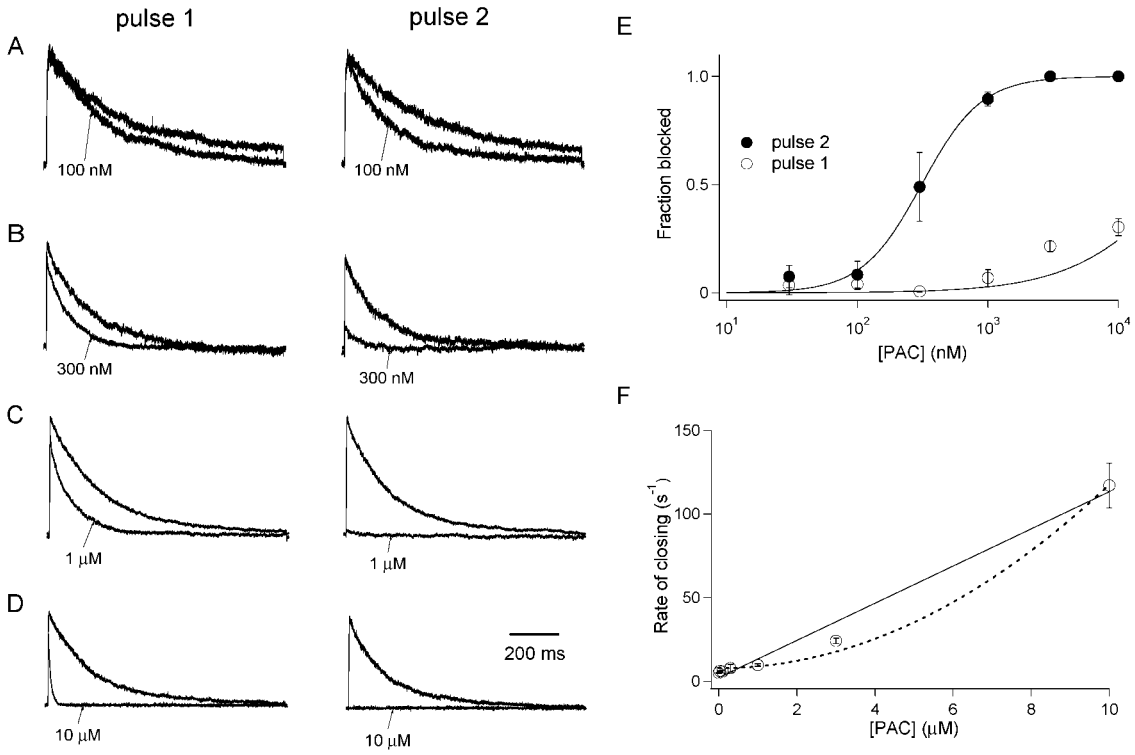

FIGURE 4: Effects of PAC on amplitude and decay rate of $K_v1.3$ channels in human T-lymphocytes. The dual pulse protocol shown in Figure 3 was repeated at different PAC concentrations. Example recordings of pulse 1 and pulse 2 from four cells are shown in (A), where control data and data recorded from the same cell after 9 min in the presence of different concentrations of PAC are plotted. These experiments were repeated with a single determination for each cell, and average block of peak currents is plotted in (E) (○, pulse 1, and ●, pulse 2), with three to four cells measured at each concentration. From these data, the rate of closing in pulse 1 was calculated as the time constant of current decay and plotted against PAC concentration in (F).

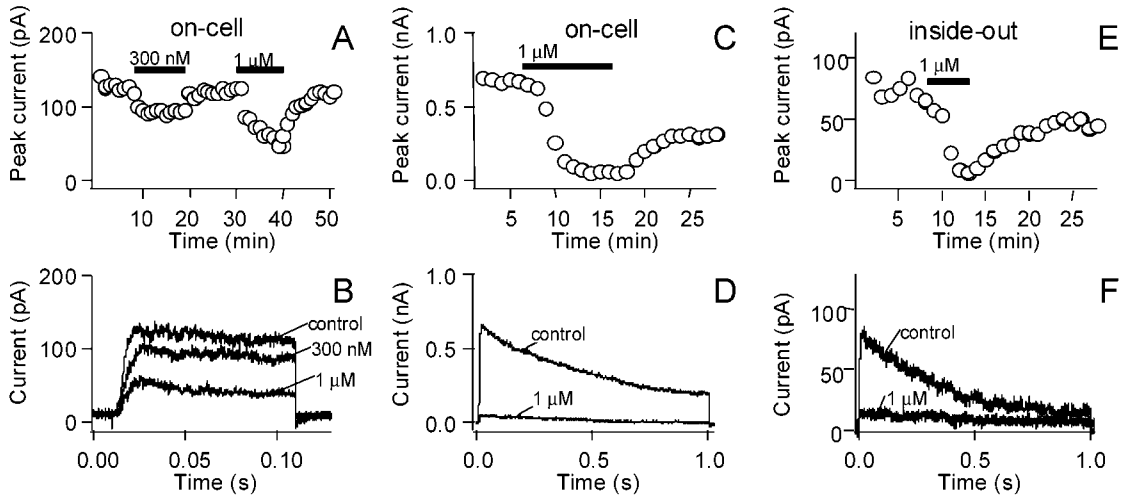

FIGURE 5: Location of the PAC binding site. Patch recordings were made in on-cell (A−D) and excised inside-out (E and F) patches from CHO cells expressing $K_v1.3$ channels. PAC was bath applied at the indicated times. Patch membrane potential was held at −80 mV with pulses to +20 mV once per minute. Bath solutions contained high potassium to zero the cell membrane potential. The same patch is shown in on-cell (C and D) and excised inside-out (E and F) recording modes.

receptor and enzyme systems was determined. When tested in ^{86}Rb efflux protocols to determine if it would block other members of the $K_v1.x$ family of channels, PAC inhibited $K_v1.1$, $K_v1.2$, $K_v1.5$, and $K_v1.6$ with very similar potencies as had been found for $K_v1.3$ (IC_{50}'s of 200−400 nM). Thus, no selectivity is observed for block of K_v1 family channels by this compound. However, when compared to its $K_v1.3$ inhibitory activity, PAC was at least 20−30-fold weaker as a blocker of $K_v2.1$ or $K_v3.2$ channels transiently expressed in COS-7 cells in voltage clamp or of smooth muscle, large conductance, calcium-activated potassium channels incorporated in lipid bilayers. Weak effects of this compound were observed on the rapid (IKr; $IC_{50} = 26$ μM) and slow (IKs; $IC_{50} = 22$ μM) components of the delayed rectifier potassium current in guinea pig cardiac myocytes, as assessed by whole cell voltage clamp. There was no significant effect of PAC (30 μM) on the inward rectifying potassium channel in this preparation. PAC (5 μM) had no effect on voltage-gated sodium channels (rat brain IIA) stably expressed in CHO cells in voltage clamp experiments. PAC did not affect L-type

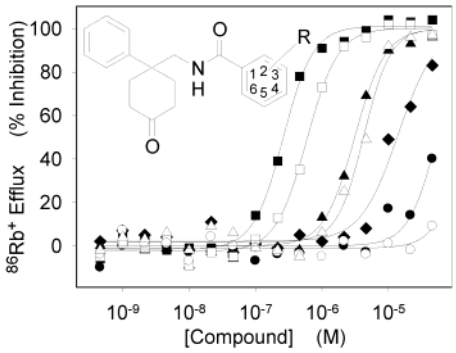

FIGURE 6: $^{86}Rb^+$ efflux from CHO/K_v1.3 cells. CHO cells stably transfected with K_v1.3 were loaded with $^{86}Rb^+$ and incubated in the absence or presence of increasing concentrations of either PAC (■) or the following compounds where R is 2-$NHCH_3$ (□), 2-OCH_2-COOH (▲), 2,4-OCH_3 (△), 2-SCH_3 (◆), H (●), or 3-OCH_3 (○). Efflux was initiated by addition of high potassium buffer in the presence of test compounds, and cells were incubated at room temperature for 15 min. Inhibition of $^{86}Rb^+$ efflux was assessed relative to the MgTX-sensitive component of an untreated control.

calcium channels, based on lack of effects at 100 μM against [^{3}H]diltiazem and [^{3}H]PN200 binding to cardiac sarcolemmal membranes. In addition, no activity was detected against CNS ligand-gated chloride channels; PAC (10 μM) did not affect either GABA- or glycine-gated chloride channels expressed in oocytes and had no effect on [^{3}H]ivermectin binding to rat brain synaptosomal plasma membranes up to 100 μM. Evaluation of PAC (10 μM) in a PanLabs biochemical and discovery screen, consisting of 132 distinct enzyme and receptor binding assays, was also conducted. Out of all of these assays, PAC was only active in three: bradykinin B1 (IC_{50} ca. 10 μM), peripheral benzodiazepine receptor (IC_{50} ca. 300 nM), and monoamine uptake (IC_{50} ca. 1 μM). Thus, PAC displays a high degree of specificity as a blocker of the K_v1 family of ion channels. A similar specificity and K_v1 selectivity profile had been determined previously for correolide (*9*).

Chemical Modifications. Chemical modification of PAC has been explored at two positions and has generated a series of disubstituted cyclohexyl (DSC) analogues. First, the role of the 2-methoxy group in the C ring was evaluated for its contribution to K_v1.3 inhibitory activity. There is a very strict structure−activity relationship regarding the substitution at this position, as few modifications are tolerated (Figure 6, Table 1). For instance, elimination of the methoxy group causes greater than 100-fold decrease in potency, but substitution of an ethoxy group is well tolerated. Several substitutions at the 2-phenyl position yielded compounds with 5−20-fold lower inhibitory activity than the parent compound (Figure 6, Table 1), whereas other substitutions, such as F, Cl, Br, I, methyl, ethyl, OCF_3, NO_2, and OCH_2CH_2OH, led to compounds that had no inhibitory activity at 30 μM (data not shown). The position of the methoxy group in the phenyl ring is also critical for conferring inhibitory activity. When the methoxy group is substituted at either the 3 or 4 position, the molecule is inactive. Double methoxy substitutions also cause loss of activity (Figure 6, Table 1). Together, these data suggest that the methyl ether may be functioning as a hydrogen bond acceptor, and they predict a specific ligand−K_v1.3 interaction.

Table 1: Inhibition of $^{86}Rb^+$ Efflux through K_v1.3 Channels by PAC Analogues[a]

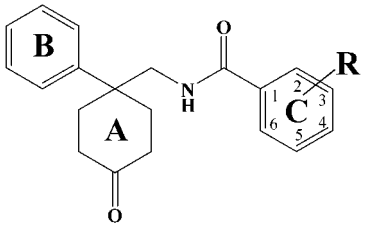

R	IC_{50} (nM)	R	IC_{50} (nM)
2-OCH_3	260	2-SCH_3	14000
H	40%[b]	2-$NHCH_3$	600
2-OCH_2CH_3	580	2-$N(CH_3)_2$	4300
2-OH	2470	3-OCH_3	9%[b]
2-OCH_2COOH	3000	2,4-OCH_3	4300

[a] Experimental conditions are described in the text, and IC_{50} values are presented. [b] Indicates the maximum inhibitory activity of a compound at 46 μM.

Table 2: Inhibition of $^{86}Rb^+$ Efflux through K_v1.3 Channels by DSC Stereoisomers[a]

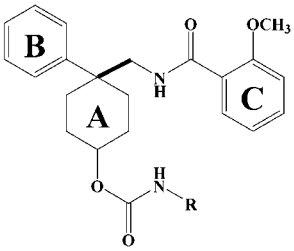

R	IC_{50} (nM) cis	IC_{50} (nM) trans	R	IC_{50} (nM) cis	IC_{50} (nM) trans
H	120	120	Ph	120	40%[b]
CH_3	150	55	CH_2Ph	150	1700
$(CH_2)_2CH_3$	100	50	$(CH_2)_2OH$	95	310
CH_2CHCH_2	115	75	$(CH_2)_2OCH_3$	145	140
$(CH_2CHCH_2)_2$	205	890			

[a] Experimental conditions are described in the text, and IC_{50} values are presented. [b] Indicates the maximum inhibitory activity of a compound at 46 μM.

Reduction of the C-1 ketone in the A ring was used to generate trans (down) and cis (up) DSC isomer pairs. A number of *trans*- and *cis*-*N*-carbamoyloxy-substituted analogues have been prepared at this position (Table 2). The K_v1.3 blocking activity of cis derivatives appears to be quite insensitive to the nature of the *N*-carbamoyloxy substituent. In contrast, there is a well-defined structure−activity relationship with the trans derivatives. As the size of the *N*-carbamoyloxy substitution is increased past a certain chain length, or made more bulky, a progressive decrease in inhibitory activity is observed with the resulting analogue. There is about a 1000-fold range in the potencies of the *N*-carbamoyloxy-substituted trans isomers examined. The most potent compound in this series is the *trans*-*N*-propylcarbamoyloxy derivative (compound **3**, Table 2), which displays an IC_{50} of 50 nM in the K_v1.3 $^{86}Rb^+$ efflux assay, ca. 5−6-fold more potent than the PAC parent compound. The *trans*-*N*-allylcarbamoyloxy analogue (compound **4**, Table 2), which was also more potent than the parent compound in the K_v1.3 $^{86}Rb^+$ efflux assay, was evaluated

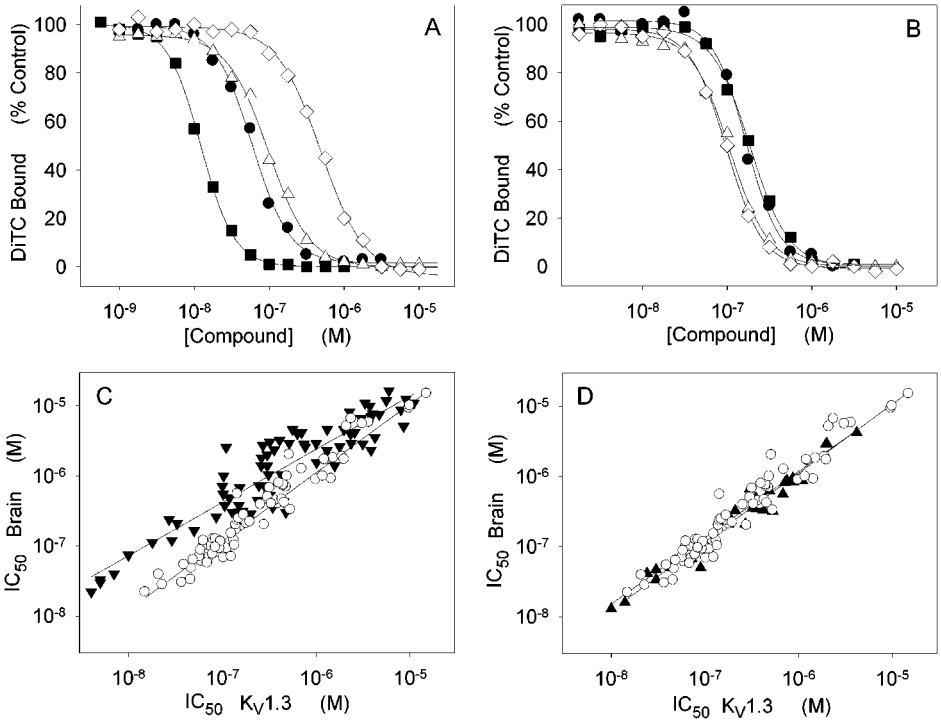

FIGURE 7: Binding of diTC to $K_v1.3$ and human brain membranes. (A and B) Membranes prepared from either human brain tissue (●, ◇) or HEK cells stably transfected with homomultimeric $K_v1.3$ channels (■, △) were incubated with 5 nM diTC in the absence or presence of increasing concentrations of either compound **1** (closed symbols) or compound **2** (open symbols) until equilibrium was achieved. Inhibition of binding was assessed relative to an untreated control. Data in (A) and (B) are from either trans or cis isomers, respectively. Compound **1**: R = $(CH_2)_2CH_3$, Table 2. Compound **2**: R = $(CH_2)_2OH$, Table 2. (C and D) Membranes prepared from either human brain tissue or HEK cells stably transfected with $K_v1.3$ were incubated with diTC in the absence or presence of increasing concentrations of PAC analogues until equilibrium was achieved. Inhibition of binding was assessed relative to an untreated control. IC_{50} values for inhibition of diTC binding in brain vs $K_v1.3$ for cis (○) and trans (▼) isomers (C) and either cis derivatives (○) or compounds with no stereochemistry at the C1 ketone group in ring A (▲) (D) are presented. Data can be fit to straight lines with an R^2 of (○) 0.94, (▼) 0.85, or (▲) 0.95.

in electrophysiological experiments in human T cells using the dual pulse protocol shown in Figures 3 and 4. The second pulse was inhibited with a K_i of 29 nM, while the first pulse was not appreciably blocked (9%) at up to 300 nM.

Although the chemical nature and the substitution pattern in the C ring are both critical determinants for producing channel blocking activity, it is possible to replace the C ring with other moieties and maintain potency. For example, replacement of the 2-methoxyphenyl group with either benzofuran or dihydrobenzofuran substituents results in analogues that inhibit $K_v1.3$ with similar potency as the parent compound (data not shown). However, regardless of the chemical nature of the inhibitor within the DSC structural series, Hill coefficients for inhibition of $^{86}Rb^+$ efflux are always ca. 2 (Figure 6 and data not shown). These data are a further indication of multiple DSC binding sites on $K_v1.3$ channels.

Modulation of DiTC Binding to $K_v1.x$ Channels by DSC Analogues. It has previously been shown that, under equilibrium conditions, diTC binds with similar affinity to all members of the $K_v1.x$ channel family but that the kinetics of ligand binding are faster to channels, such as $K_v1.3$ and $K_v1.4$, that undergo C-type inactivation (*18*). To determine if these newly identified inhibitors interact with K_v1 channels at the diTC receptor, binding of diTC was monitored to membranes derived from cells expressing homotetrameric $K_v1.3$ channels or human brain tissue, which consists primarily of $K_v1.1/K_v1.2$-containing heteromultimeric channels (*9*, *19*). Panels A and B of Figure 7 show the results of such experiments carried out with two pairs of trans (A) or cis (B) DSC derivatives, each containing the 2-methoxyphenyl substitution. In all cases, there is complete concentration-dependent inhibition of diTC binding, and the Hill coefficients for inhibition are close to 2. For comparison, inhibition of diTC binding by correolide displays a Hill coefficient of 1 (*9*, *18*). Cis DSC derivatives do not display any apparent selectivity as inhibitors of diTC binding when $K_v1.3$ and brain $K_v1.x$ channels are compared (Figure 7B). However, trans DSC derivatives are more potent as inhibitors of diTC binding to $K_v1.3$ than to the heteromultimeric $K_v1.x$ channels present in brain (Figure 7A). This diTC binding inhibitory pattern is characteristic of all trans- and cis-isomer pairs that have been investigated. Figure 7C presents a correlation plot of IC_{50} values for inhibition of diTC binding to either $K_v1.3$ or human brain membranes by 73 different pairs of DSC analogues. These data can be fit to two independent linear regressions with different slopes, depending of the type of DSC isomer examined. Extrapolation of these relations predicts that trans-isomer derivatives could have ca. a 10-fold higher affinity for $K_v1.3$ channels than for the $K_v1.x$ channels present in human brain, whereas cis-isomer derivatives do not discriminate at all between these two types of channels. In addition, compounds that do not possess a chiral center at the C-1 position, such as the parent compound PAC, behave like cis-isomer derivatives in terms of their inhibitory pattern (Figure 7D). Thus, it appears that a trans-isomer substitution at the C-1 position of the A ring can confer some specificity toward an interaction with $K_v1.3$ channels. Consistent with this idea, the *trans-N*-allylcarbamoyloxy analogue derived from PAC (compound **4**, Table 2)

displays a small selectivity window for inhibition of $^{86}Rb^+$ efflux from $K_v1.3$ vs $K_v1.2$ expressing cell lines, in that it is 2−4-fold more potent against $K_v1.3$. It is interesting to note that, out of the other $K_v1.x$ channels investigated in diTC binding protocols (e.g., $K_v1.1$, $K_v1.2$, $K_v1.4$, $K_v1.5$, and $K_v1.6$), $K_v1.4$ channels display a similar selectivity profile as $K_v1.3$ channels with respect to inhibition of diTC binding by this structural series. Such a profile could be related to a common feature of $K_v1.3$ and $K_v1.4$ channels, as both undergo C-type inactivation.

Modulation of ^{125}I-HgTX$_1$A19Y/Y37F Binding to $K_v1.x$ Channels by DSC Analogues. Ion channels are multi-drug receptor complexes where binding sites for inhibitors can either overlap, be allosterically coupled, or be completely independent. For instance, correolide, which binds in the central cavity on the C-terminal side of the selectivity filter of $K_v1.3$ channels, does not affect binding of peptidyl inhibitors to the outer vestibule of this channel (*9*). To determine whether the DSC class of $K_v1.3$ channel inhibitors affects binding of peptide channel blockers, the interaction of ^{125}I-HgTX$_1$A19Y/Y37F with membranes containing $K_v1.3$ channels was evaluated in the absence or presence of selected test compounds. Figure 8A presents data obtained with the same two pairs of DSC isomeric analogues evaluated in Figure 7A,B. Trans derivatives exhibit a much larger degree of ^{125}I-HgTX$_1$A19Y/Y37F binding inhibition than cis derivatives, which clearly behave as partial inhibitors of peptide binding. The same pattern has been observed with all pairs of chiral C-1 analogues examined (data not shown). Furthermore, none of the analogues lacking a stereochemical center at the C-1 position of the A ring inhibit ^{125}I-HgTX$_1$A19Y/Y37F binding to $K_v1.3$.

^{125}I-HgTX$_1$A19Y/Y37F binds with high affinity to homomultimeric $K_v1.1$, $K_v1.2$, and $K_v1.3$ channels, as well as to those heteromultimeric $K_v1.x$ channels present in brain membranes (*19*). None of the compounds investigated in the DSC series, regardless of the stereochemistry at the C-1 position, have any effect on the interaction of ^{125}I-HgTX$_1$A19Y/Y37F with $K_v1.1$, $K_v1.2$, or either human or rat brain membranes (Figure 8B and data not shown). Thus, inhibition of ^{125}I-HgTX$_1$A19Y/Y37F binding by trans derivatives is only observed with $K_v1.3$ membranes. These data strongly suggest that the peptide and small molecule inhibitors bind to different sites on the channel. In addition, these data suggest that the features governing the interaction of trans DSC derivatives with $K_v1.3$ channels are different from those in other $K_v1.x$ channels and that these differences are manifested in a $K_v1.3$-specific allosteric interaction between the receptor for the trans DSC isomeric derivatives and the peptidyl inhibitors. It is worth noting that although cis DSC derivatives do not have a pronounced effect on ^{125}I-HgTX$_1$A19Y/Y37F binding to $K_v1.3$ channels, they are able to modulate the interaction of trans-isomer analogues with the channel. For example, in the presence of 10 μM *cis-N*-propylcarbamoyloxy or 3 μM *cis-N*-allylcarbamoyloxy DSC analogues (compounds **3** and **4**, Table 2), the dose−response curve for the trans congener is parallel shifted 100- and 10-fold to the right, respectively (data not shown). These data imply that both isomers bind to the same site on the channel but that the allosteric interaction with the ^{125}I-HgTX$_1$A19Y/Y37F receptor depends on the orientation of the substituent at the C-1 chiral center of the A ring.

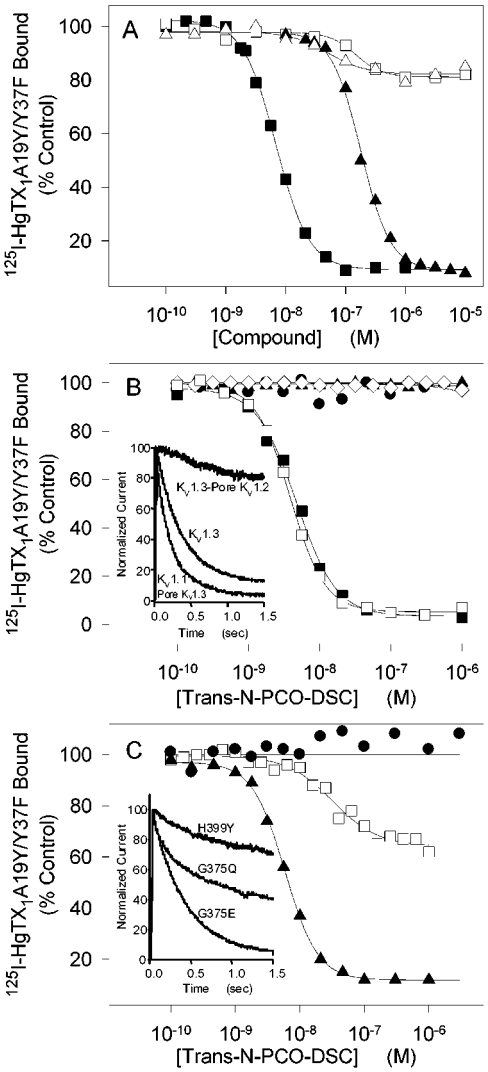

FIGURE 8: Binding of ^{125}I-HgTX$_1$A19Y/Y37F to $K_v1.x$ channels. (A) Membranes prepared from HEK cells stably transfected with $K_v1.3$ were incubated with 0.2 pM ^{125}I-HgTX$_1$A19Y/Y37F in the absence or presence of increasing concentrations of either trans (■, ▲) or cis isomers (□, △) for 20 h at room temperature. Inhibition of binding was assessed relative to an untreated control [■, □, R = $(CH_2)_2CH_3$, Table 2; ▲, △, R = $(CH_2)_2OH$, Table 2]. (B and C) Interaction of trans-isomer cyclohexanes with $K_v1.3$: role of C-type inactivation. (B) Membranes derived from either TsA-201 cells transiently transfected with $K_v1.3$-p$K_v1.2$ (●) or $K_v1.1$-p$K_v1.3$ (□) or HEK cells stably expressing $K_v1.1$ (▲), $K_v1.2$ (◇), or $K_v1.3$ (■) were incubated with 0.2 pM ^{125}I-HgTX$_1$A19Y/Y37F in the absence or presence of increasing concentration of the *trans-N*-propylcarbamoyloxy DSC analogue (*trans-N*-PCO-DSC). Inhibition of binding was assessed relative to an untreated control. Inset: currents evoked by a voltage step to +20 mV from a holding potential of −80 mV in CHO cells transiently transfected with either $K_v1.3$, $K_v1.3$−p$K_v1.2$, or $K_v1.1$−p$K_v1.3$. (C) Membranes derived from TsA-201 cells transiently transfected with either $K_v1.3$H399Y (●), $K_v1.3$G375Q (□), or $K_v1.3$G375E (▲) were incubated with 0.2 pM ^{125}I-HgTX$_1$A19Y/Y37F in the absence or presence of increasing concentrations of *trans-N*-PCO-DSC for 20 h at room temperature. Inhibition of binding was assessed relative to an untreated control. Inset: currents evoked by a voltage step to +20 mV from a holding potential of −80 mV in CHO cells transiently transfected with either $K_v1.3$H399Y, $K_v1.3$G375Q, or $K_v1.3$G375E.

Binding of DSC Inhibitors to $K_v1.3$: Role of C-Type Inactivation. Results from both diTC and ^{125}I-HgTX$_1$A19Y/Y37F binding studies suggest that trans DSC derivatives may differentially associate with channels that undergo C-type

inactivation. To test this idea, two chimeric channels were constructed; in one, $K_v1.1-pK_v1.3$, the pore region of $K_v1.3$ was transferred to the noninactivating channel, $K_v1.1$, while in the other, $K_v1.3-pK_v1.2$, the pore region of $K_v1.2$ was substituted with that of $K_v1.3$. When these chimeric channels are transiently expressed in CHO cells, the resulting currents elicited by a depolarizing 200 ms pulse from −80 to +20 mV either do not inactivate (i.e., $K_v1.3$-$pK_v1.2$) or display a time−course of inactivation similar to that of $K_v1.3$ (i.e., $K_v1.1-pK_v1.3$) (see inset, Figure 8B). Thus, C-type inactivation appears to be governed by specific residues within the pore region of $K_v1.3$, as has previously been described (*25*−*27*). ^{125}I-HgTX$_1$A19Y/Y37F binds to all of these channels with the same affinity (K_d = 0.1−0.3 pM; data not shown). Consistent with the idea that C-type inactivation affects the binding characteristics of the trans DSC isomers, compound **3** (Table 2), *trans-N*-propylcarbamoyloxy DSC, inhibits ^{125}I-HgTX$_1$A19Y/Y37F binding to $K_v1.1-pK_v1.3$ but not to $K_v1.3-pK_v1.2$ (Figure 8B). To further investigate the correlation between binding of trans DSC isomers and C-type channel inactivation, single point mutants of $K_v1.3$ with different C-type inactivation kinetics were constructed. $K_v1.3$ (His^{399}Tyr) and $K_v1.3$ (Gly^{375}Gln) channels inactivate slower than native channels, whereas $K_v1.3$ (Gly^{375}Glu) has nearly the same kinetics of inactivation as wild-type $K_v1.3$ (see inset, Figure 8C). Binding of ^{125}I-HgTX$_1$A19Y/Y37F to $K_v1.3$ (Gly^{375}Glu) is modulated by the *trans-N*-propylcarbamoyloxy DSC analogue with similar characteristics as found for $K_v1.3$ (Figure 8C). However, characteristics of peptide binding inhibition to the other two mutant channels by this compound are much different; both extent and concentration dependence of inhibition are shifted with the Gly^{375}Gln mutant, and the allosteric coupling between sites appears to be absent in the His^{399}Tyr mutant. These data illustrate that the specific allosteric interaction of trans DSC derivatives with HgTX$_1$A19Y/Y37F binding to $K_v1.3$ channels correlates with the rates of C-type channel inactivation and suggest a potential mechanism for achieving selectivity of inhibitor action within this family of voltage-gated potassium channels.

Inhibition of Human T Cell Proliferation in Vitro by DSC Analogues. In human T cells, blockade of the $K_v1.3$ channel either by peptidyl inhibitors, such as charybdotoxin or MgTX, or by correolide suppresses T cell activation (*6*, *10*, *28*). This can be demonstrated using two different paradigms. First, the functional effects of the DSC class of $K_v1.3$ inhibitors were evaluated in T cell proliferation assays where activation is triggered by anti-CD3 and irradiated PBMC. PAC and the *trans-N*-propylcarbamoyloxy and *trans-N*-allylcarbamoyloxy DSC analogues produce concentration-dependent inhibition of [^{3}H]thymidine uptake into human T cells (Figure 9). Importantly, inhibition by all three compounds is reversed by addition of conditioned medium from PHA-activated T cells, which contains a variety of cytokines (Figure 9 and data not shown). These data indicate that the inhibitory activity is specific and not due to general cytotoxicity of the compounds, except at 20 μM, the highest concentrations of the latter two compounds tested, where reversal was not observed. The pattern of inhibition observed with all three compounds is similar to that produced by MgTX (*6*) and correolide (*10*), except for the concentration of these newly identified $K_v1.3$ inhibitors that is needed to elicit the inhibitory response. Second, the production of IL-2, stimulated by PMA and ionomycin after 24 h, was monitored in the absence or presence of these three compounds. All three inhibited IL-2 production with similar concentration dependencies as found for their effects on T cell proliferation (data not shown). However, none of these agents blocked anti-CD28 stimulation of IL-2 production (i.e., a non-calcium-dependent pathway), which is a key indication of the specificity with which members of the DSC series function. Similar IL-2 blocking patterns have been observed for MgTX and correolide as well (*6*, *10*).

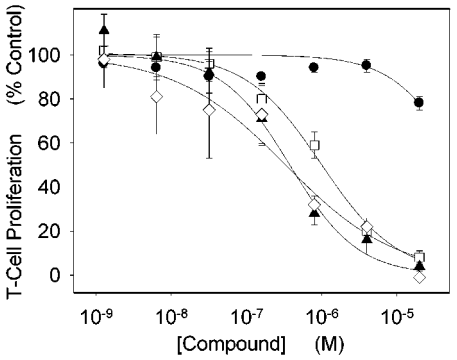

FIGURE 9: Inhibition of human T cell proliferation. Purified T cells were stimulated with anti-CD3 in the absence or presence of increasing concentrations of either PAC (□), *trans-N*-propylcarbamoyloxy DSC (▲), or *trans-N*-allylcarbamoyloxy DSC (◇). Inhibition of [^{3}H]thymidine uptake was assessed relative to an untreated control. T cell proliferation in the presence of exogenous IL-2 (●) is not inhibited by PAC. (□) IC_{50} = 1 μM, data represent the mean ± SEM of seven different donors; (▲) IC_{50} = 340 nM, data represent the mean ± SEM of four different donors; (◇) IC_{50} = 360 nM, data represent the mean ± SEM of two different donors.

DISCUSSION

The results reported in this study represent the first description of a series of 4,4-disubstituted cyclohexyl compounds as potent and selective blockers of the K_v1 family of potassium channels. The parent compound in this series, 4-phenyl-4-[3-(2-methoxyphenyl)-3-oxo-2-azaprop-1-yl]cyclohexanone (PAC), blocks $K_v1.3$ channels in both flux and electrophysiological assays with a potency of about 300 nM and a Hill coefficient near 2. This Hill coefficient suggests that two or more molecules of PAC, or other DSC molecules in this series, participate in blocking a single $K_v1.3$ channel. This property has not been observed with other known organic K_v1 channel blockers (*9*, *12*−*14*, *29*−*31*). Block of $K_v1.3$ channels by PAC and related analogues follows a defined structure−activity relationship; a 6-fold enhancement in potency was obtained within the currently reported series. As expected for specific blockers of $K_v1.3$ channels, these compounds reversibly inhibit proliferation of human T cells, without displaying cytotoxicity or blocking Ca^{2+}-independent T cell stimulation pathways. Thus, the DSC series has in vitro immunosuppressant activity. Although PAC does not display inhibitor selectivity within the K_v1 family of channels, modification of the cyclohexyl template at the C-1 position generates trans- (down) isomer analogues that display distinct interaction patterns with $K_v1.3$ and $K_v1.4$ vs other $K_v1.x$ channels in biochemical binding assays. This property correlates with the ability of channel types to undergo C-type inactivation.

The findings that selective peptidyl blockers of $K_v1.3$ channels inhibit Ca^{2+}-dependent T cell activation in in vitro

assays (*6*, *28*, *32*) and suppress immune responses in an in vivo animal model (*6*, *7*) have provided validation that the $K_v1.3$ channel is a therapeutic target for immunosuppression. Since peptides are not ideal drug candidates, a search for small molecules that display suitable characteristics has been undertaken by several groups. WIN 17317-3 is the first small molecule inhibitor of $K_v1.3$ to be described (*14*). This agent appears to interact potently with the C-type inactivated state of $K_v1.3$ and $K_v1.4$ channels and selectively blocks these channels compared with other K_v channels (*13*). However, WIN 17317-3 also blocks voltage-gated sodium channels with high affinity (*17*), and this deleterious feature prevents development of WIN 17317-−3 as an immunosuppressant. A structurally unrelated inhibitor of $K_v1.3$ channels, UK-78282, has also been identified (*12*). UK-78282 preferentially blocks C-type inactivated channels, and it appears to bind in a region that corresponds to the internal pore of the channel. UK-78282 was shown to inhibit human T cell proliferation in in vitro assays (*12*), but this activity was not reversed by exogenous application of cytokines, suggesting that UK-78282 also possesses additional cellular actions (unpublished observations).

Correolide is the first identified potent, small molecule, natural product inhibitor of $K_v1.3$ (*8*, *9*). Correolide selectively blocks members of the K_v1 family of potassium channels, and it specifically blocks the calcium-dependent pathway for T cell activation (*10*). A radiolabeled derivative, diTC, binds with similar high affinity to all $K_v1.x$ channels, but kinetics of binding correlate with the rates of C-type inactivation of these channels (*18*). Recently, the binding domain for diTC on $K_v1.3$ channels has been characterized by site-directed mutagenesis (*23*). DiTC appears to bind in the pore, on the cytoplasmic side of the selectivity filter, and high-affinity binding may result from a complementary shape between diTC and that region of the channel. Interestingly, some of the residues that contribute to the high-affinity diTC receptor in $K_v1.3$ channels are present in a region of the protein that undergoes conformational changes during gating (*33*−*36*). The features that provide high-affinity and specific interactions between diTC and $K_v1.3$ channels may result from processes, such as C-type inactivation, which are not present in many other voltage-gated K^+ channels. Members of this family of compounds have been shown to attenuate the delayed-type hypersensitivity reaction to tuberculin in in vivo experiments performed in mini-swine (*10*). However, correolide and some analogues promote acetylcholine release from peripheral nerve endings in the enteric nervous system of the ileum, possibly due to blocking presynaptic $K_v1.1$ channels that modulate neurotransmitter release (*37*). This additional site of action may account for some of the limited, temporary toxicity (i.e., diarrhea) observed in vivo with these $K_v1.3$ channel inhibitors. There is a clear need to identify new structural classes of $K_v1.3$ inhibitors that are more appropriate candidates for immunosuppressive drug development. In this context, the results presented in this study disclose the identity of a new chemical class of small molecule $K_v1.3$ inhibitors that blocks T cell activation in vitro in a specific fashion.

The parent compound, PAC, was identified using the same functional assay that led to the discovery of correolide. Although both compounds display similar potencies in flux and electrophysiological assays, the Hill coefficients for channel inhibition differ. In the flux assays, correolide displays a n_H of 1, whereas PAC and its analogues have n_H near 2. Hill coefficients of 2 have also been observed for these compounds in their inhibition of diTC and ^{125}I-$HgTX_1$A19Y/Y37F binding to $K_v1.3$ channels. These data suggest the presence of multiple binding sites for PAC in $K_v1.3$. This is in marked contrast to correolide, which binds in a 1:1 stoichiometry to $K_v1.3$ channels (*9*).

PAC reversibly blocks currents through $K_v1.3$ channels in human T-lymphocytes. Block occurred after bath application in whole cell, on-cell, and excised inside-out patch experiments, suggesting that the binding site is accessible from the intracellular or membrane compartments. Channel block was negligible in the absence of depolarizing pulses that open and inactivate channels, suggesting that conformational changes occurring in the channel during depolarization are required for drug binding. Another alternative explanation, such as depolarization enhancing drug block because of voltage-dependent binding, seems unlikely because PAC is uncharged and cannot directly sense the membrane field. Thus, resting states of $K_v1.3$ channels are poorly blocked by PAC, while channel states (open or inactivated) occurring following depolarization can be blocked. Some characteristics of channel block by PAC are consistent with a mechanism where PAC binds to and blocks open channels. PAC clearly shortens the burst times of channels opened during a depolarizing pulse. The time course of channel closing during a depolarizing pulse was monoexponential at all PAC concentrations, and the apparent rate of PAC block of open channels continuously increased, with no indication of saturation, as PAC concentration was raised. PAC may bind to inactivated channels, but the data provide no direct support for or against this mechanism. Binding of PAC to sites in the pore accessible from the cytoplasmic side could prevent potassium flux from the cytoplasmic compartment to the selectivity filter. In the presence of low (physiological) concentrations of external potassium, this would lead to low occupancy of potassium sites in the selectivity filter and enhanced C-type inactivation, as occurs for small organic potassium channel blockers (*29*). In this way, functional coupling between pore block by PAC and C-type inactivation can occur.

The structure−activity relationship for $K_v1.3$ channel inhibition by this new class of blockers is interesting. The position and nature of substitutions in the C ring are both critical for maintaining channel blocking activity. Repositioning the methoxy group at a locus other than the 2 position of the phenyl ring eliminates activity, and other chemically distinct substitutions at that position decrease activity as well, suggesting that this region of PAC is important for high-affinity interaction with $K_v1.3$ channels. However, it is possible to replace the entire phenyl ring with other ring systems, such as benzofuran or dihydrobenzofuran moieties, without suffering great loss in activity. Another region of the molecule that is important for the interaction of DSC analogues with $K_v1.x$ channels is the C-1 position of the cyclohexanone ring. Reduction of the C-1 ketone group generates a number of *N*-carbamoyloxy analogues that can be resolved as either trans (down) or cis (up) isomers. These stereo isomers interact with the $K_v1.3$ channel in a well-defined fashion. With cis isomers, both small and large substitutions are well tolerated, suggesting a minor role for

this region of the molecule in its interaction with the channel. In marked contrast, trans-isomer derivatives only tolerate small alkyl chain substitutions; larger or bulkier substitutions cause large decreases in the channel blocking activity of this series. It is possible that, for the trans derivatives, the presence of either large or bulky substituents prevents access of the inhibitor to its binding site. Alternatively, these substituents could lead to destabilization of the channel-bound state in a stereospecific manner.

The trans- and cis-isomer pairs also display significant differences in terms of their interactions with other $K_v1.x$ channels. For a given pair of isomers, trans derivatives can be 10-fold more potent in inhibiting binding of diTC to $K_v1.3$ channels than to human brain $K_v1.x$ channels, whereas cis derivatives do not distinguish between these channel types. The apparent specificity of this interaction is reminiscent of a pattern previously found with diTC, although, in that latter case, the kinetics of ligand binding, but not the affinity of the ligand, were found to differ among different $K_v1.x$ channels (*18*). However, in both cases, channels with relatively fast C-type inactivation, such as $K_v1.3$ and $K_v1.4$, display either higher affinity for the trans isomers or faster binding kinetics for diTC.

The correlation between C-type inactivation and the effects of trans-isomer DSC analogues recurs when monitoring the allosteric interaction between these compounds and peptidyl inhibitors that bind in the outer vestibule of the channel. Although ^{125}I-HgTX$_1$A19Y/Y37F binds with similar high affinity to homomultimeric $K_v1.1$, $K_v1.2$, or $K_v1.3$ channels and heteromultimeric $K_v1.x$ channels present in brain, trans-isomer DSC analogues only inhibit binding of the peptide to $K_v1.3$ channels. The ability of trans-isomer DSC derivatives to affect ^{125}I-HgTX$_1$A19Y/Y37F binding to $K_v1.3$ channels depends on the C-type inactivation properties of this channel, as supported by the results obtained with $K_v1.x$ mutants that display altered C-type inactivation kinetics. The results of binding experiments are consistent with the idea that the specific channel conformations associated with C-type inactivation are responsible for the distinct features of trans DSC isomer interactions with $K_v1.3$ channels. Although the mechanism by which C-type inactivation confers specificity to the interaction of the trans DSC isomer with the channel has not been elucidated, these data suggest that it may be possible to exploit this property for achieving functional selectivity between potassium channels.

The DSC class of $K_v1.3$ inhibitors mimics the activity of peptides and correolide in in vitro human T cell proliferation assays, suggesting that it represents a novel type of immunosuppressant agent. The properties of these molecules suggest two important avenues for improvement: their small size should allow more facile chemical modification than has been possible with a large complex natural product, such as correolide; trans-isomer derivatives display some forms of specificity toward $K_v1.3$ over other $K_v1.x$ channels. Improving the characteristics of the DSC series may lead to the identification of an analogue with appropriate pharmacokinetic and pharmacological properties for consideration as a drug development candidate.

ACKNOWLEDGMENT

We thank Drs. Hartmut Glossmann and Hans-Guenther Knaus, University of Innsbruck, Austria, for supplying human brain tissue from which membranes were prepared. We also thank Drs. Charles Cohen, Joung Goulet, Armando Lagrutta, Joseph Salata, Peter Sinclair, MacHardy Smith, Martin Springer, Keith Wafford, and Richard Brochu, Mark Holmes, Jane Hong, Jessica Liu, Kashmira Shah, Jixin Wang, and Frederick Wong for synthetic chemistry, selectivity assays, and experimental support.

REFERENCES

1. Cahalan, M. D., and Chandy, K. G. (1997) *Curr. Opin. Biotechnol. 8*, 749−756.
2. Kaczorowski, G., and Koo, G. C. (1994) *Perspect. Drug Discovery Des. 2*, 233.
3. Helms, L. M. H., Felix, J. P., Bugianesi, R. M., Garcia, M. L., Stevens, S., Leonard, R. J., Knaus, H.-G., Koch, R., Wanner, S. G., Kaczorowski, G. J., and Slaughter, R. S. (1997) *Biochemistry 36*, 3737−3744.
4. Leonard, R. J., Garcia, M. L., Slaughter, R. S., and Reuben, J. P. (1992) *Proc. Natl. Acad. Sci. U.S.A. 89*, 10094−10098.
5. Lin, C. S., Boltz, R. C., Blake, J. T., Nguyen, M., Talento, A., Fischer, P. A., Springer, M. S., Sigal, N. H., Slaughter, R. S., Garcia, M. L., Kaczorowski, G. J., and Koo, G. C. (1993) *J. Exp. Med. 177*, 637−645.
6. Koo, G. C., Blake, J. T., Talento, A., Nguyen, M., Lin, S., Sirotina, A., Shah, K., Mulvany, K., Hora, D. A., Jr., Cunningham, P., Wunderler, D. L., McManus, O. B., Slaughter, R., Bugianesi, R., Felix, J., Garcia, M., Williamson, J., Kaczorowski, G., Sigal, N. H., Springer, M. S., and Feeney, W. (1997) *J. Immunol. 158*, 5120−5128.
7. Beeton, C., Barbaria, J., Giraud, P., Devaux, J., Benoliel, A.-M., Gola, M., Sabatier, J. M., Bernard, D., Crest, M., and Beraud, E. (2001) *J. Immunol. 166*, 936−944.
8. Goetz, M. A., Hensens, O. D., Zink, D. L., Borris, R. P., Morales, F., Tamayo-Castillo, G., Slaughter, R. S., Felix, J., and Ball, R. G. (1998) *Tetrahedron Lett. 39*, 2895−2898.
9. Felix, J. P., Bugianesi, R. M., Schmalhofer, W. A., Borris, R., Goetz, M. A., Hensens, O. D., Bao, J.-M., Kayser, F., Parsons, W. H., Rupprecht, K., Garcia, M. L., Kaczorowski, G. J., and Slaughter, R. S. (1999) *Biochemistry 38*, 4922−4930.
10. Koo, G. C., Blake, J. T., Shah, K., Staruch, M. J., Dumont, F., Wunderler, D., Sanchez, M., McManus, O. B., Sirotina-Meisher, A., Fischer, P., Boltz, R. C., Goetz, M. A., Baker, R., Bao, J., Kayser, F., Rupprecht, K. M., Parsons, W. H., Tong, X.-C., Ita, I. E., Pivnichny, J., Vincent, S., Cunningham, P., Hora, D., Jr., Feeney, W., Kaczorowski, G., and Springer, M. S. (1999) *Cell. Immunol. 197*, 99−107.
11. Vianna-Jorge, R., Oliveira, C. F., Garcia, M. L., Kaczorowski, G. J., and Suarez-Kurtz, G. (2000) *Br. J. Pharmacol. 131*, 772−778.
12. Hanson, D. C., Nguyen, A., Mather, R. J., Rauer, H., Koch, K., Burgess, L. E., Rizzi, J. P., Donovan, C. B., Bruns, M. J., Canniff, P. C., Cunningham, A. C., Verdries, K. A., Mena, E., Kath, J. C., Gutman, G. A., Cahalan, M. D., Grissmer, S., and Chandy, K. G. (1999) *Br. J. Pharmacol. 126*, 1707−1716.
13. Nguyen, A., Kath, J. C., Hanson, D. C., Biggers, M. S., Canniff, P. C., Donovan, C. B., Mather, R. J., Bruns, M. J., Rauer, H., Aiyar, J., Lepple-Wienhues, A., Gutman, G. A., Grissmer, S., Cahalan, M. D., and Chandy, K. G. (1996) *Mol. Pharmacol. 50*, 1672−1679.
14. Hill, R. J., Grant, A. M., Volberg, W., Rapp, L., Faltynek, C., Miller, D., Pagani, K., Baizman, E., Wang, S., Guiles, J. W., and Krafte, D. S. (1995) *Mol. Pharmacol. 48*, 98−104.
15. Chandy, K. G., DeCoursey, T. E., Cahalan, M. D., McLaughlin, C., and Gupta, S. (1984) *J. Exp. Med. 160*, 369−385.
16. Rauer, H., and Grissmer, S. (1996) *Mol. Pharmacol. 50*, 1625−1634.
17. Wanner, S. G., Glossman, H., Knaus, H.-G., Baker, R., Parsons, W., Rupprecht, K. M., Brochu, R., Cohen, C. J., Schmalhofer, W., Smith, M., Warren, V., Garcia, M. L., and Kaczorowski, G. J. (1999) *Biochemistry 38*, 11137−11146.
18. Hanner, M., Schmalhofer, W. A., Green, B., Bordallo, C., Liu, J., Slaughter, R. S., Kaczorowski, G. J., and Garcia, M. L. (1999) *J. Biol. Chem. 274*, 25237−25244.
19. Koschak, A., Bugianesi, R. M., Mitterdorfer, J., Kaczorowski, G. J., Garcia, M. L., and Knaus, H.-G. (1998) *J. Biol. Chem. 273*, 2639−2644.

20. Hamill, O. P., Marty, A., Neher, E., Sakmann, B., and Sigworth, F. J. (1981) *Pfluegers Arch. 391*, 85−100.
21. Ho, S. N., Hunt, H. D., Horton, R. M., Pullen, J. K., and Pease, L. R. (1989) *Gene 77*, 51−59.
22. Hanner, M., Vianna-Jorge, R., Kamassah, A., Schmalhofer, W. A., Knaus, H.-G., Kaczorowski, G. J., and Garcia, M. L. (1998) *J. Biol. Chem. 273*, 16289−16296.
23. Hanner, M., Green, B., Gao, Y.-D., Schmalhofer, W. A., Matyskiela, M., Durand, D. J., Felix, J. P., Linde, A.-R., Bordallo, C., Kaczorowski, G. J., Kohler, M., and Garcia, M. L. (2001) *Biochemistry 40*, 11687−11697.
24. Grissmer, S., and Cahalan, M. (1989) *Biophys. J. 55*, 203−206.
25. Panyi, G., Sheng, Z., Tu, L. W., and Deutsch, C. (1995) *Biophys. J. 69*, 896−903.
26. Liu, Y., Jurman, M. E., and Yellen, G. (1996) *Neuron 16*, 859−867.
27. Yellen, G., Sodickson, D., Chen, T.-Y., and Juman, M. E. (1994) *Biophys. J. 66*, 1068−1075.
28. Price, M., Lee, S. C., and Deutsch, C. (1989) *Proc. Natl. Acad. Sci. U.S.A. 86*, 10171−10175.
29. Baukrowitz, T., and Yellen, G. (1996) *Science 271*, 653−656.
30. Baukrowitz, T., and Yellen, G. (1996) *Proc. Natl. Acad. Sci. U.S.A. 93*, 13357−13361.
31. Yellen, G., Jurman, M. E., Abramson, T., and MacKinnon, R. (1991) *Science 251*, 939−942.
32. Kalman, K., Pennington, M. W., Lanigan, M. D., Nguyen, A., Rauer, H., Mahnir, V., Paschetto, K., Kem, W. R., Grissmer, S., Gutman, G. A., Christian, E. P., Cahalan, M. D., Norton, R. S., and Chandy, K. G. (1998) *J. Biol. Chem. 273*, 32697−32707.
33. del Camino, D., and Yellen, G. (2001) *Neuron 32*, 649−656.
34. del Camino, D., Holmgren, M., Liu, Y., and Yellen, G. (2000) *Nature 403*, 321−325.
35. Holmgren, M., Shin, K. S., and Yellen, G. (1998) *Neuron 21*, 617−621.
36. Liu, Y., Holmgren, M., Jurman, M. E., and Yellen, G. (1997) *Neuron 19*, 175−184.
37. Suarez-Kurtz, G., Vianna-Jorge, R., Pereira, B. F., Garcia, M. L., and Kaczorowski, G. J. (1999) *J. Pharmacol. Exp. Ther. 289*, 1517−1522.

BI025722C